PNAS
www.pnas.org

Supplementary Information for

IDO1 scavenges reactive oxygen species in myeloid-derived suppressor cells to prevent graft-*versus*-host disease

Ji Min Ju, Giri Nam, Young-Kwan Lee, Minho Jung, Hanna Chang, Woojin Kim, Woo Jeong Shon, Ji Young Lim, Joo Young Kim, Jun Chang, Chang Ki Min, Dong Sup Lee, Kyungho Choi, Dong-Mi Shin, Eun Young Choi

Corresponding author:

Eun Young Choi (E-mail: eycii@snu.ac.kr)

Dong-Mi Shin (E-mail: shindm@snu.ac.kr)

This PDF file includes:

Supplemental methods

GVHD induction

CD45.1$^+$ IDO-KO or WT mice were used as BM and T cell donors. T cell-depleted BM (TCD-BM) and splenic T cells were prepared by magnetic-activated cell sorting (MACS) according to the manufacturer's instructions (Miltenyi Biotec, Auburn, CA, USA), as described previously (1). For induction of GVHD, BALB.B and B6D2F1 mice were irradiated with 900 and 1,100 cGy, respectively, of a ^{137}Cs source with split doses at 5-h intervals. TCD-BM (5×10^6) and T cells (3×10^6) were injected into the tail vein 5 h after irradiation. In neutrophil-depletion experiment, an anti-Ly6G Ab (1A8; BioXcell, Lebanon, NH, USA) or isotype control rat IgG2a (BioXell) was injected intraperitoneally to IDO-KO-BM and WT-BM hosts (250 μg/mouse) on days 4 and 8 post-transplantation.

Cell staining and flow cytometry

Leukocytes were prepared from peripheral blood, lymphoid organs, and non-lymphoid organs and stained for flow cytometric analysis, as described in detail previously (2). The antibodies used were FITC- and APC-conjugated anti-CD4 (GK1.5; eBioscience, San Diego, CA, USA) and anti-CD8 (53-6.7; eBioscience) monoclonal antibodies, respectively. Other monoclonal antibodies used included eFluor 450 anti-Ly6G (RB6-8C5; eBioscience), FITC anti-CD115 (AFS98; eBioscience), PE anti-CD25 (PC61.5, eBioscience), PE anti-CD124 (I015F8, BioLegend, San Diego, CA, USA), PE anti-CD244 (m2B4 (B6)458.1; BioLegend), APC anti-Ly6c (HK1.4; eBioscience), PE-Cy5 anti-F4/80 (BM8; BioLegend), PE-Cy7 anti-CD11b (M1/70; eBioscience), eFluor 450 anti-Ly6G (RB6-8C5; eBioscience), FITC anti-CD115 (AFS98; eBioscience), PE anti-CD25 (PC61.5; eBioscience), PE anti-CD124 (I015F8; BioLegend), PE anti-CD244 (m2B4 (B6)458.1; BioLegend), APC anti-Ly6c (HK1.4; eBioscience), PE-Cy5 anti-F4/80 (BM8; BioLegend), PE-Cy7 anti-CD11b (M1/70; eBioscience), APC anti-IFN-γ (XMG1.2; eBioscience), PE anti-IL-17A (TC11-18H10; BD

Biosciences, San Diego, CA), PE-Cy7 anti-CD101 (Moushi101, eBioscience), and PE anti-Foxp3 (FJK-16s; eBioscience).

BM cell culture and immunosuppression assay

Gr-1$^+$ cells were MACS-purified from spleens of GVHD hosts or BM cell culture. BM cells depleted of T and B cells by MACS were cultured for 4 days in the presence of GM-CSF (40 ng/mL, PeproTech, Rocky Hill, NJ, USA) or supplemented with LPS (1 μg/mL; Sigma-Aldrich, St. Louis, MO, USA) overnight 1 day before harvest. NAC (N-acetylcysteine; Sigma-Aldrich) or BSO (L-buthionine-*S, R*-sulfoximine; Sigma-Aldrich) was added to GM-CSF culture at 1 mM concentration for the ROS-scavenging or -inducing experiment, respectively. For immunosuppression assay, MACS-purified T cells were labeled with carboxyfluorescein diacetate succinimidyl ester (CFSE; 2.5 μM; Invitrogen, Carlsbad, CA, USA), and stimulated with anti-CD3 (2 μg/mL; 145-2C11, BD Biosciences)/CD28 (1 μg/mL; 37.51, BD Biosciences) antibodies. After 72 h of co-culture with Gr-1$^+$ cells at a 1:1 ratio, T cells were analyzed for CFSE dilution by flow cytometry. Suppression is expressed as the percentage of undivided CFSE (Gr-1$^+$ cells) compared with that of the control (-), calculated using the equation [(% diluted CSFE labeled T cells only − % diluted CFSE-labeled T cells with Ly6G$^+$ cells) ÷ % diluted CFSE-labeled T cells only] × 100.

Transcriptome analysis

Gr-1$^+$ (Ly6G$^+$) cells MACS-purified from splenocytes on day 7 after allogeneic (or syngeneic) BMT were used for RNA extraction when the purity was higher than 97%. For microarray hybridization, total RNA was isolated and purified using a DNA-free RNA isolation kit (RNAqueous-4PCR kit; Ambion, Austin, TX, USA). RNA samples were first amplified for array analysis using the Illumina Total Prep RNA Amplification Kit (Ambion), as described previously (1). Amplified cRNA (1.5 μg) was hybridized on Mouse WG-6 v2 Expression BeadChip arrays (Illumina, San Diego, CA, USA), containing more than 45,281 well-annotated Ref transcripts. The array chips were scanned on a BeadArray reader (BeadStation 500G; Illumina) and subjected to gene identification and quantitation using Genome Studio software (v. 1.0.2.; Illumina).

Bioinformatics analysis of gene expression profiles

The raw microarray data were pre-processed through three steps: i) background correction was performed, and ii) the data were log-transformed to log2 scale and iii) normalized by the quantile normalization method implemented in Genome Studio software (Illumina). Significant differences among the groups were identified by analysis of variance (ANOVA; FDR < 5%) of log2-transformed normalized data using Partek® Genomics Suite (v. 6.3; Partek, St Louis, MO, USA). The DEGs were categorized based on their biological functions by GO analysis. GSEA was performed to examine the significance of the enrichment of the biological subsets of interest in the whole gene expression profile (http://www.broadinstitute.org/gsea/index.jsp). Hierarchical clustering analysis was performed with Genesis software (v. 1.7.5) using the Pearson correlation distance with the average linkage algorithm. Significant pathways were analyzed using the tools of Ingenuity® Pathway Analysis (IPA; Qiagen, Redwood City, CA, USA). Transcriptome data of MDSCs from patients with allo-HSCT were provided by Lee *et al.* (3). Gene expression correlations were analyzed by Pearson's correlation coefficient.

Measurement of ROS levels

The intracellular ROS level was measured using CellROX-Green (Life Technologies, Gaithersburg, MD, USA) according to the manufacturer's instructions. Cells were labeled with 5 μM CellROX-Green cell-permeable dye, incubated at 37°C for 20 min, washed, and stained with antibodies for flow cytometry. ROS levels are presented as the mean fluorescence intensity (MFI) of CellROX-Green. Extracellular H_2O_2 was detected using the Amplex Red Hydrogen Peroxide Assay Kit (Invitrogen). The H_2O_2 concentration was determined using a working solution of 100 μM Amplex Red reagent and 0.2 U/mL horseradish peroxidase (HRP) for 30 min. Fluorescence was measured with excitation and emission at 560 and 590 nm, respectively, using an Infinite 200 Pro Plate Reader (Tecan, Männedorf, Switzerland).

Retroviral plasmid DNA construction and transduction

The coding sequence for the full-length hu-IDO was cloned into the pMSCV-IRES-GFP (pMIG) retroviral expression vector (Addgene plasmid #9044, a gift from William Hahn) designated pMIG-hIDO1 (WT). A heme-binding mutant (H346A; histidine replaced by alanine at p346) and catalytic mutant (F226A; phenylalanine replaced by alanine at p226) were constructed by PCR-based site-directed mutagenesis using 5'-CTGAGGAGCTACGCCCTGCAAATC-3' (forward), 5'-GATTTGCAGGGCGTAGCTCCTCAG-3' (reverse) and 5'-CCAAAGCAGCC TTCAGTGTTCTTCG-3' (forward), 5'-CGAAGAACACTGAAGGCTGCT TTT GG-3' (reverse) primers, respectively. All mutated genes were cloned into the pMIG vector and verified by DNA sequencing. The retroviral plasmids and a plasmid encoding VSV-G cDNA (pMD.G) were transiently transfected into Phoenix GP cells. Culture supernatant containing VSV-G pseudotyped retrovirus was used for the transduction of Phoenix Eco cells to produce ecotropic retroviruses. Green fluorescent protein (GFP)-positive Phoenix Eco cells were FACS-sorted (FACSAria III; BD Biosciences) to generate stable cell lines. The culture supernatant containing ecotropic retrovirus was harvested and concentrated 10-fold for the transduction of mouse BM cells. TCD-BM cells from IDO-KO mice were cultured in the presence of GM-CSF (40 ng/mL; Primegene, Shanghai, China), SCF (20 ng/mL; Primegene), IL-3 (20 ng/mL; Primegene), and IL-6 (50 ng/mL; Primegene) and, 24 h later, transduced with the concentrated retroviruses by spin-infection in the presence of polybrene (6 μg/mL, Sigma-Aldrich). The spin infection was repeated on days 3 and 4 post-BM differentiation. Transduction efficiency was measured by flow cytometric analysis of GFP expression.

Quantification of heme and kynurenine

The supernatant from *in vitro* cultured BM cells was passed through a Microcon Centrifugal Filter with an Ultracel YM-3 column (Millipore, Billerica, MA, USA) (60 min at 14°C, 21,000*g*) to remove proteins (MW > 3 kDa). The heme level in protein-depleted supernatant was measured using a QuantiChrom heme assay kit (Bioassay Systems, Hayward, CA, USA) according to the manufacturer's instructions. The catalytic activity of hu-IDO and its mutants was measured by

colorimetric Kyn assay. In brief, an aliquot of culture supernatant concentration or mouse serum was treated with 30% trichloroacetic acid (Sigma-Aldrich) for 30 min at 50°C to hydrolyze N-formylkynurenine to Kyn and then mixed with freshly prepared Ehrlich's reagent (2% 4-dimethylamino benzaldehyde in glacial acetic acid; Tokyo Chemical Industry, Tokyo, Japan). The absorbance at 492 nm was measured using a microplate reader (BioTek, Winooski, VT, USA) with Gen5 software (BioTek) after incubation for 10 min.

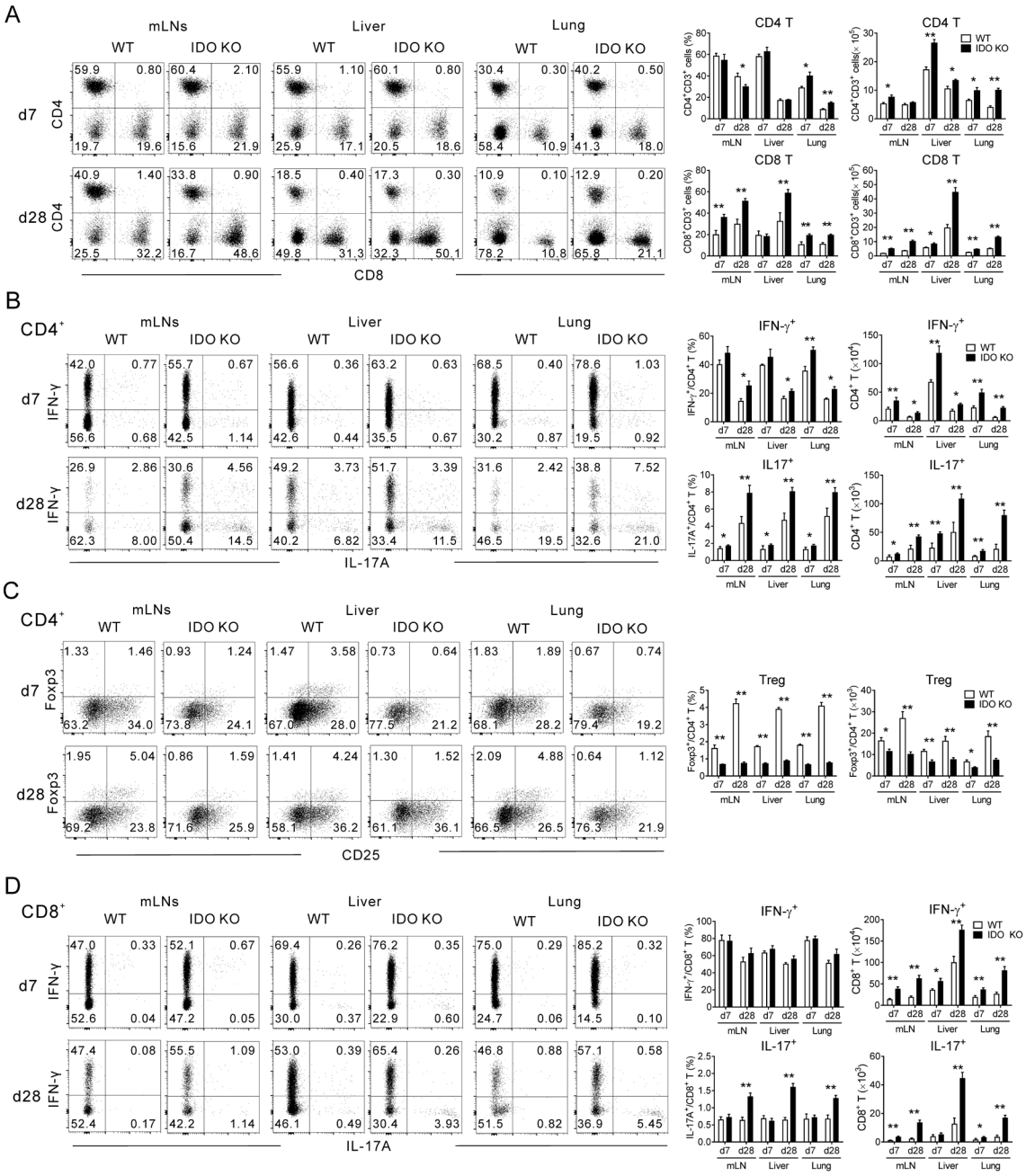

Fig. S1. Enhanced alloimmunity of T cells in organs from IDO1 KO GVHD hosts. Flow cytometric analysis of the mLNs, liver, and lung from allogeneic BALB.B hosts on days 7 and 28 post-transplantation. (*A*) Representative CD4 (PE/Cy5) and CD8 (APC/Cy7) flow cytometry profiles of

mLNs, liver, and lung are shown with gating on live CD45.1$^+$ cells. The frequencies and numbers of CD45.1$^+$ CD4$^+$ and CD8$^+$ T cells are plotted. (*B*) Representative IFN-γ and IL-17A flow cytometry profiles of mLNs, liver, and lung are shown with gating on CD45.1$^+$CD4$^+$ T cells. The percentages and numbers of IFN-γ- and IL-17A-producing CD4$^+$ T cells are plotted. (*C*) Representative Foxp3 and CD25 flow cytometry profiles of mLNs, liver, and lung are shown with gating on CD45.1$^+$CD4$^+$ T cells. The percentages and numbers of CD25$^+$Foxp3$^+$CD4$^+$ Tregs are plotted. (*D*) Representative IFN-γ (APC) and IL-17A (PE) flow cytometry profiles of mLNs, liver, and lung are shown with gating on CD45.1$^+$CD8$^+$ T cells. The percentages and numbers of IFN-γ- and IL-17A-producing CD45.1$^+$CD8$^+$ T cells are plotted. Data (*A*-*D*) are representative of three independent experiments (n = 3/group/experiment) and are presented as means ± SEM (*$P < 0.05$, **$P < 0.01$ as determined by Student's *t*-test).

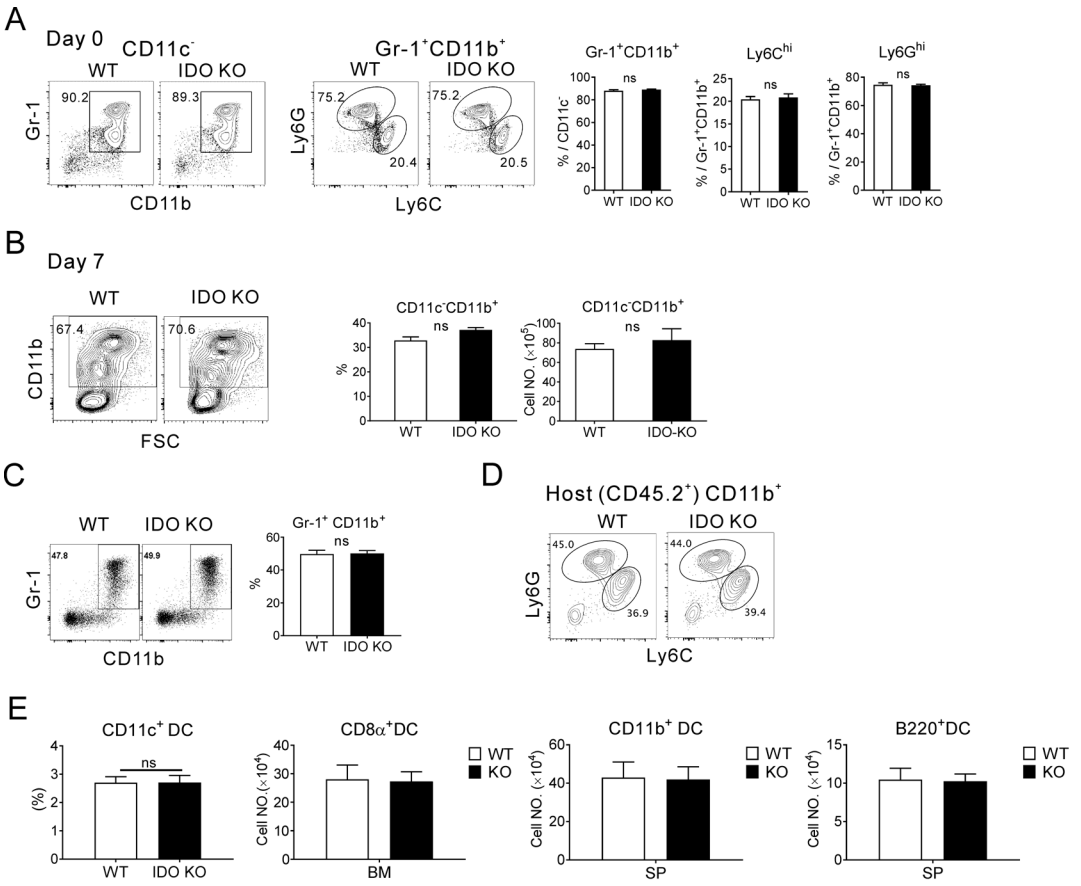

Fig. S2. CD11c$^-$CD11b$^+$ myeloid cells and CD11c$^+$ DCs in IDO-KO-BM and WT-BM GVHD hosts. (*A*) Flow cytometric analysis of TCD-BM cells for transplantation (Day 0). Representative CD11b/Gr-1 (Ly6G) profile of CD11c$^-$ cells and Ly6C/y6G profiles of Gr-1$^+$CD11b$^+$ cells in IDO-KO and WT BM transplants are shown. Percentages of Gr-1$^+$CD11b$^+$ cells in CD11c$^-$ cells, and Ly6C^{hi} and Ly6G^{hi} cells in Gr-1$^+$CD11b$^+$ cells are plotted. (*B-D*) Flow cytometric analysis of myeloid cells in the spleens of WT-BM and IDO-KO-BM hosts (BALB.B) on day 7 post-transplantation. Representative (*B*) CD11b/FSC and (*C*) CD11b/Gr-1 (Ly6G) profiles of splenocytes are shown with gating on CD45.2$^-$CD11c$^-$ cells. Percentages and numbers of CD11c$^-$CD11b$^+$ cells, and percentages of Gr-1$^+$CD11b$^+$ cells are plotted. (*D*) Composition of host residual Gr-1$^+$CD11b$^+$ cells in the spleens. Representative Ly6C/Ly6G profiles of CD45.2$^+$CD11b$^+$ cells are shown. (*D*) Percentages of whole (CD45.2$^-$) CD11c$^+$ DCs in the spleen, and numbers of DC subsets in bone marrow (BM) or spleen (SP) are plotted. Data (*A*–*E*) are representative of at least three independent experiments (n = 3/group/experiment) and are presented as means ± SEM (*P < 0.05, **P < 0.01, ***P < 0.001 as determined by Student's *t*-test).

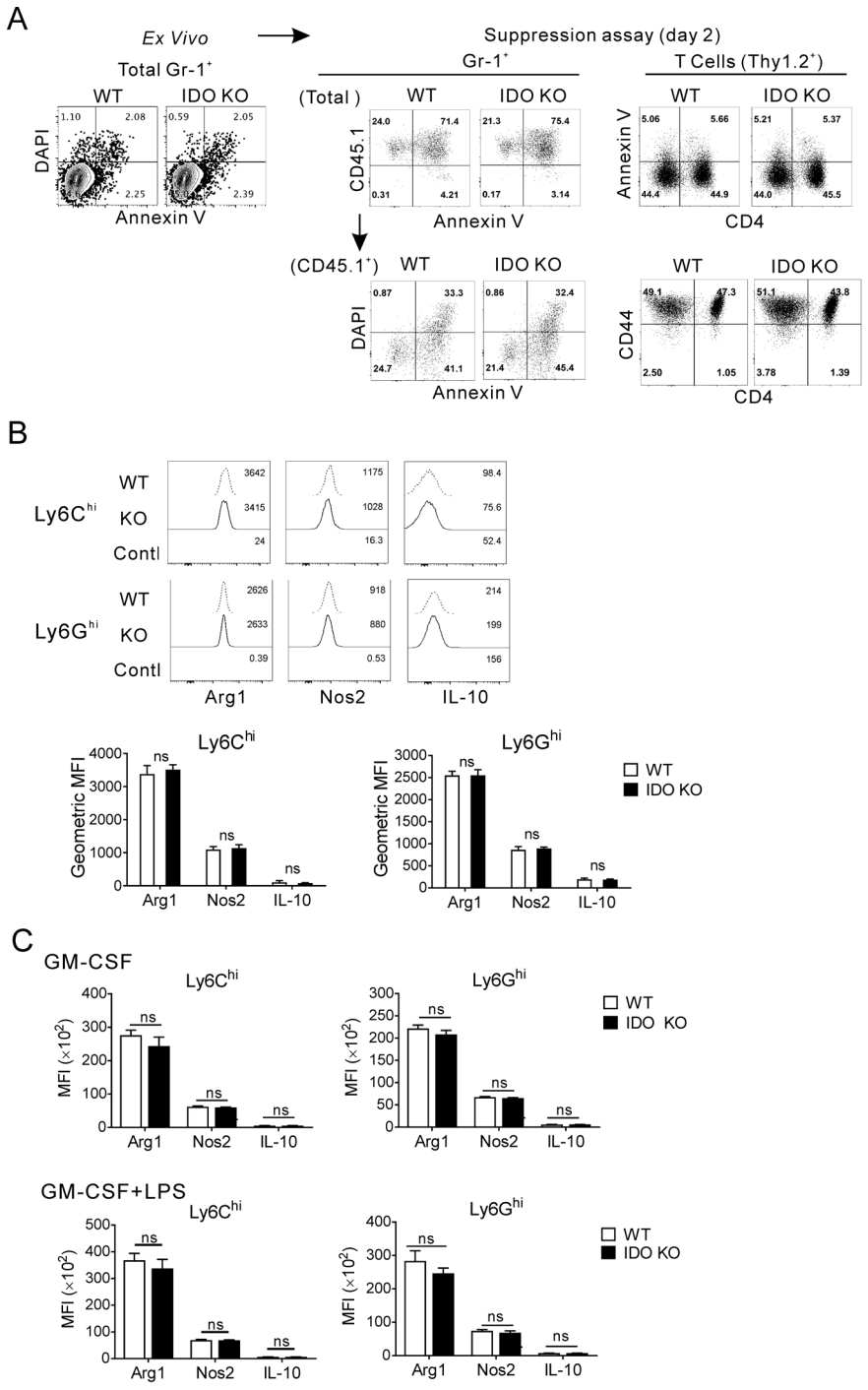

Fig. S3. Apoptosis in suppression assay, and expression of MDSC functional mediators in IDO-KO and WT Gr-1$^+$ CD11b$^+$ cells from GVHD hosts and generated *in vitro* via BM cell culture. (*A*) Apoptosis of splenic Gr-1$^+$CD11b$^+$ cells *ex vivo* from IDO-KO-BM and WT-BM hosts (BALB.B), and Gr-1$^+$CD11b$^+$ cells and T cells from suppression assay. Gr-1$^+$ cells isolated from IDO-KO-BM and WT-BM hosts on day 7 post-transplantation before suppression assay, and the Gr-1$^+$ cells co-

incubated with CD3-stimulated T cells for 2 days were stained with antibodies and Annexin-V for flow cytometry. Representative Annexin-V/CD45.1 profiles of total Gr-1$^+$ cells and DAPI/Annexin-V profiles of CD45.1$^+$Gr-1$^+$ cells are shown. T cells were gated on Thy1.2$^+$ cells (CD4 T, Thy1.2$^+$CD4$^+$ and CD8 T: Thy1.2$^+$CD4$^-$ cells). Representative Annexin-V/CD4, and CD44/CD4 profiles of Thy1.2$^+$ T cells are shown. Data represent three independent experiments (n = 3/group/experiment). (*B*) Splenic Gr-1$^+$ CD11b$^+$ cells from IDO-KO-BM and WT-BM hosts were analyzed by flow cytometry for the expression of Arg-1, iNOS, and IL-10. Representative single histograms are shown, with MFI values indicated. MFI values of the Ly6C^{hi} and Ly6G^{hi} subsets are shown. (*C*) Gr-1$^+$CD11b$^+$ cells generated *in vitro* from IDO-KO and WT BM in the presence of GM-CSF alone or together with LPS were analyzed by flow cytometry for the expression of Arg-1, iNOS, and IL-10. The MFI values of the Ly6C^{hi} and Ly6G^{hi} subsets are plotted. Data (B and C) are representative of at least three independent experiments (n = 3/group/experiment) and presented as means ± SEM (*P < 0.05, **P < 0.01, ***P < 0.001 as determined by Student's *t*-test).

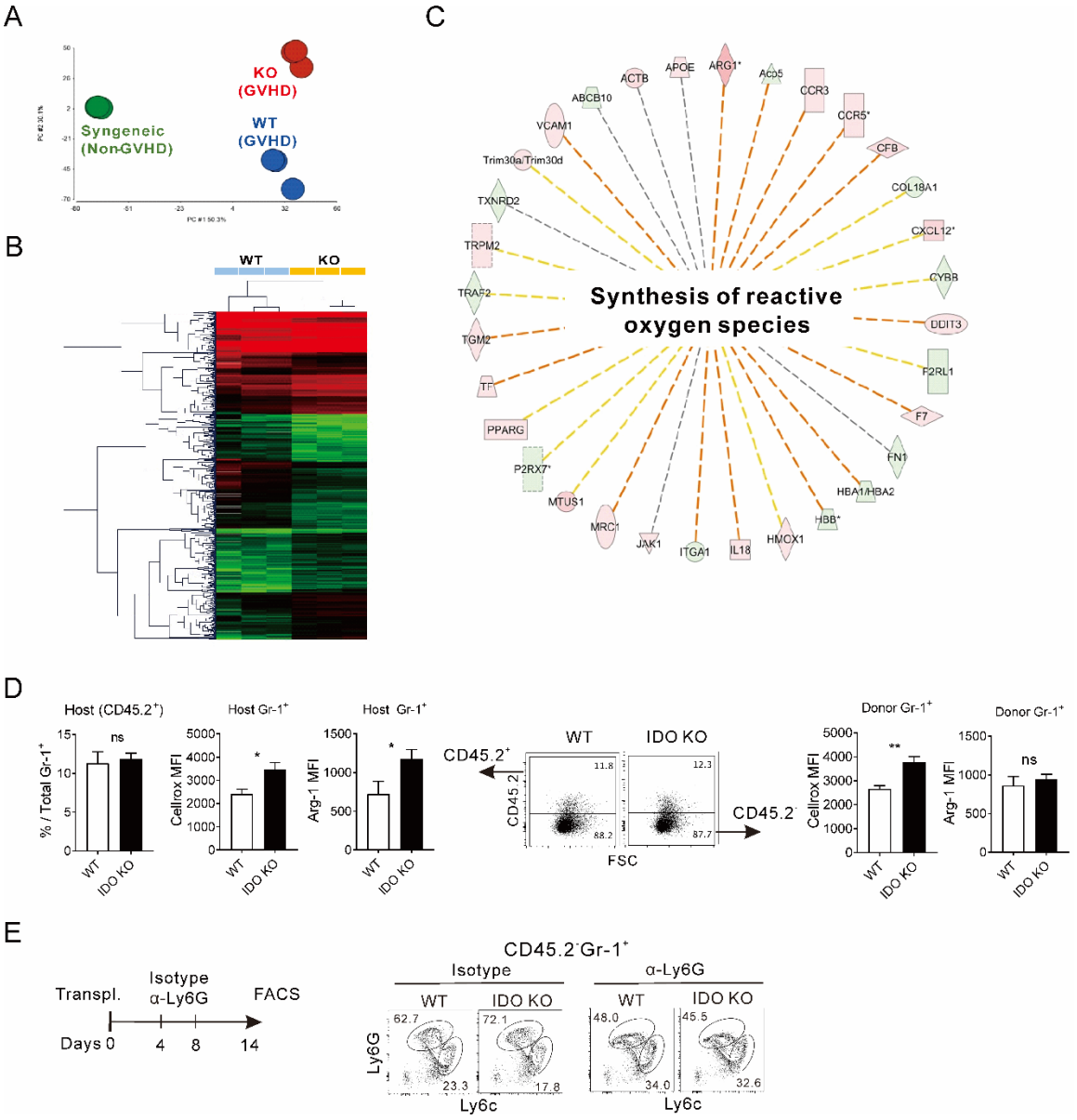

Fig. S4. Transcriptomic analysis indicates enhanced ROS and neutrophil generation in Gr-1⁺ cells from IDO-KO-BM hosts. (A) Principle component analysis (PCA) using transcriptomic data from splenic Ly6G⁺ cells from WT-BM and IDO-KO-BM hosts (BALB.B), and syngeneic (WT BM + T → B6) non-GVHD hosts on day 7 post-transplantation. (*B*) Hierarchical clustering of DEGs. Red and green represent increased and decreased gene expression, respectively. (C) In a gene ontology analysis of the DEGs, 'Synthesis of ROS' was identified as a significantly enriched function. Transcriptome data (*A* - *C*) were obtained from two independent experiments of RNA isolation, using Gr-1⁺ cells MACS-purified from three mice per group. (*D*) ROS and Arg-1 levels in host

(CD45.2$^+$) Gr-1$^+$ cells and donor-derived (CD45.2$^-$) Gr-1$^+$ cells in the spleens of IDO-KO-BM and WT-BM hosts on day 7 post-transplantation. Representative CD45.2/FSC profiles of total Gr-1$^+$CD11b$^+$ cells are shown. Proportions of CD45.2$^+$ host-derived cells in total Gr-1$^+$CD11b$^+$ cells in the spleens, and MFI values of host (CD45.2$^+$)- and donor (CD45.2$^-$)-derived Gr-1$^+$ by CellRox and Arg-1 staining are plotted. Data represent three independent experiments (n = 3/group/experiment) and are presented as means ± SEM (* $P < 0.05$, ** $P < 0.01$, *** $P < 0.001$ as determined by Student's *t*-test). (E) Neutrophil-depletion in IDO-KO-BM and WT-BM hosts. IDO-KO-BM or WT-BM hosts were injected intraperitoneally with an anti-Ly6G or isotype control Ab (250 μg/mouse) on days 4 and 8 post-transplantation. Neutrophil depletion was confirmed by flow cytometric analysis of myeloid cells in the spleens on day 14 post-transplantation when the mice were euthanized for T-cell phenotyping. Representative Ly6C/Ly6G profiles of CD45.2$^-$Gr-1$^+$ cells are shown. Data represent three independent experiments (n = 3/group/experiment).

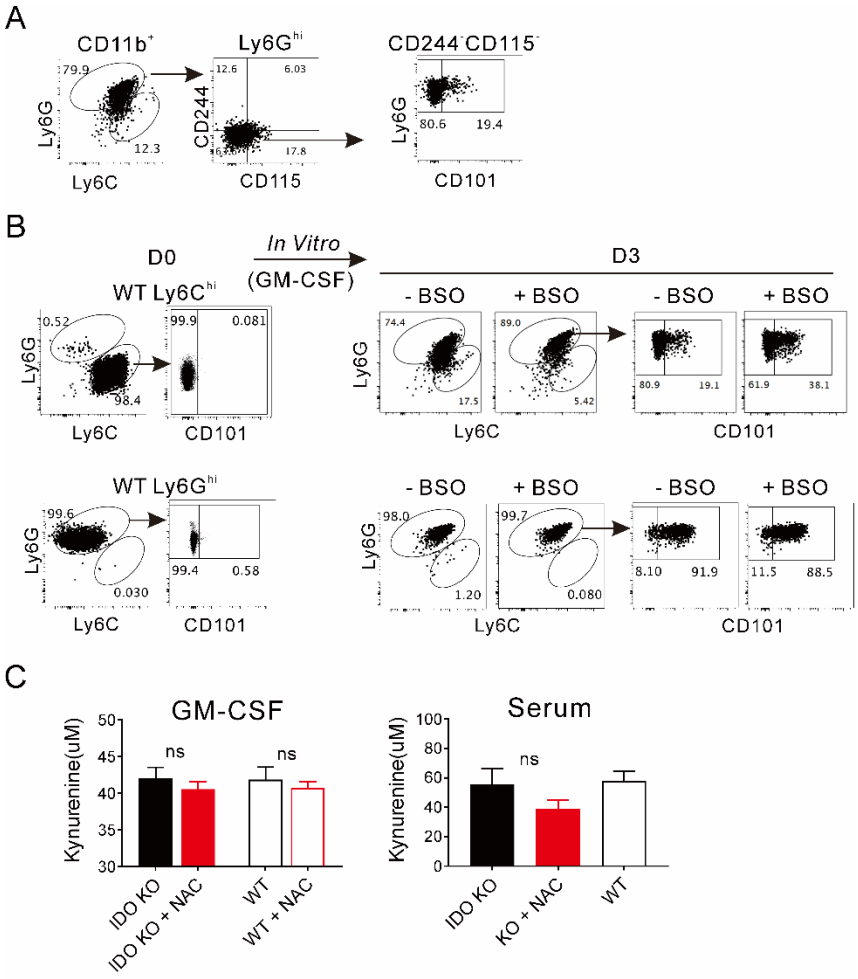

Fig. S5. Effects of ROS elevation on neutrophil generation and ROS scavenging effects on Kyn production. (*A*) Presence of CD101^{+} cells in CD244^{-}CD115^{-}Ly6G^{hi} cells. Ly6G^{hi} cells generated from FACS-sorted WT Ly6C^{hi} cells in GM-CSF culture were analyzed for expression of CD244, CD115, and CD101 after 3 days of culture. Representative Ly6C/Ly6G profile of CD11b^{+} cells, CD244/CD115 profile of Ly6G^{hi} cells, and CD101/Ly6G profile of CD244^{-}CD115^{-}Ly6G^{hi} cells are shown. (*B*) Effect of ROS elevation on the differentiation of Ly6C^{hi} and Ly6G^{hi} cells. Ly6C^{hi} and Ly6G^{hi} cells FACS-sorted from naïve WT BM were cultured in the presence of GM-CSF (40 ng/mL) alone or together with BSO (1 mM). Representative Ly6C/Ly6G and CD101/Ly6G profiles of the sorted subsets (D0), and Ly6C/Ly6G profiles of CD11b^{+} cells and Ly6G/CD101 profiles of Ly6G^{hi} subsets generated by *in vitro* culture for 3 days (D3) are shown. Data (*A* and *B*) represent three

independent experiments (n = 3/group/experiment). (*C*) Kyn levels in BM cell culture supernatant and in the serum of GVHD hosts with or without NAC treatment. NAC was treated to BM culture on day 0, or daily to IDO-KO-BM host (days 4 - 6 post-transplantation). Kyn concentrations in the culture supernatant (day 4) and serum of GVHD hosts with or without NAC treatment (day 7 post-transplantation) are plotted. Data represent three independent experiments (n = 3/group/experiment) and are presented as means ± SEM (* $P < 0.05$, ** $P < 0.01$, *** $P < 0.001$ as determined by Student's *t*-test).

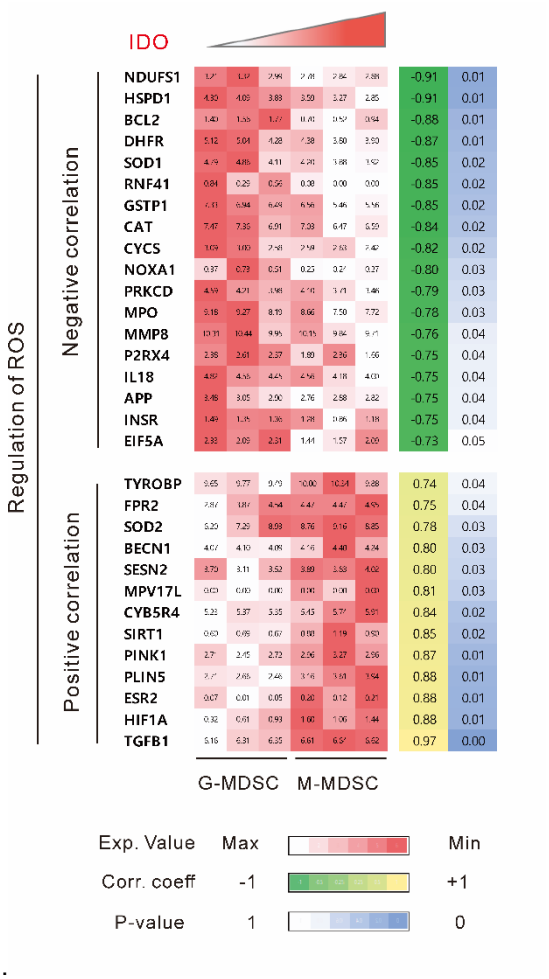

Fig. S6. Correlations of the expression levels of IDO and ROS regulation genes in M- and G-MDSCs from patients with allo-HSCT. RNA-sequencing data obtained from M- and G-MDSCs of patients with allo-HSCT (3) were analyzed. Genes involved in ROS scavenging or production were retrieved from the Gene Ontology analysis. The normalized RPKM (Reads Per Kilobase Million) value for each gene is shown (red scale). Pearson's correlation coefficient was calculated (yellow-green scale). P-values are shown in the right-most column (blue scale).

SI References

1. Lee YK*, et al.* (2018) Skewed dendritic cell differentiation of MyD88-deficient donor bone marrow cells, instead of massive expansion as myeloid-derived suppressor cells, aggravates GVHD. *Immune Netw* 18(6):e44.
2. Choi EY*, et al.* (2002) Real-time T-cell profiling identifies H60 as a major minor histocompatibility antigen in murine graft-versus-host disease. *Blood* 100(13):4259-4265.
3. Lee SE*, et al.* (2018) Matrix Metalloproteinase-9 in Monocytic Myeloid-Derived Suppressor Cells Correlate with Early Infections and Clinical Outcomes in Allogeneic Hematopoietic Stem Cell Transplantation. *Biol Blood Marrow Transplant* 24(1):32-42.